The Zlamal Approximation on a Sphere

I. G. BUROVA[1], N. A. LEBEDINSKAYA[2], D. M. LEBEDINSKI[2], V. G. KORNEEV[2]
[1]Department of Computational Mathematics, St. Petersburg State University,
7/9 Universitetskaya Embankment, St. Petersburg, 199034,
RUSSIA

[2]Department of Parallel Algorithms, St. Petersburg State University,
7/9 Universitetskaya Embankment, St. Petersburg, 199034,
RUSSIA

Abstract: - Finite element approximation is often used to solve various problems in mathematical physics, such as boundary value problems. Previously, the authors considered the Courant approximation on a sphere. The Zlamal approximation on the plane gives smaller errors of approximation than the Courant approximation. This paper discusses a generalization of the Zlamal approximation on the plane and the Zlamal approximation on a sphere. The theoretical results are given for the Zlamal approximation on the plane and the Zlamal approximation on a sphere. The errors of approximation obtained with the Zlamal approximation and with the Courant approximation are compared. The results of the numerical experiments are given.

Key-Words: - local approximation, Zlamal-type approximation, Courant-type approximation, approximation on a sphere, triangulation, basis functions

Received: June 2, 2026. Revised: July 11, 2026. Accepted: August 8, 2026. Published: November 6, 2026.

1 Introduction

In 2024, we celebrated 100 years since the birth of Professor Miloš Zlámal [1]. The most important mathematical achievements of Professor Miloš Zlámal are the study of various properties of analytical solutions of ordinary and partial differential equations and the theoretical foundation of the finite element method [2], such as the minimum angle condition and curved finite elements [3]. He also developed the mortar finite elements used to cover a strip between two different types of finite elements.

The finite element method is currently widely used for the numerical solution of boundary value problems in mathematical physics. The method is based on the concept of finite element approximation, which is a type of local approximation.

Main features of finite element approximation are:

- triangulation of the initial domain;
- local interpolation basis;
- the piecewise polynomial nature of the approximation.
- the use of variational principles for derivation of the discrete system of algebraic equations approximating the boundary value problem.

An extensive bibliography and a detailed exposition of the finite element method are contained in [4]'s monograph and [5]'s paper. We note that paper [6] is also significant in Zlamal's exploration of finite element approximation.

Review paper [7] discusses the developments in immersed or unfitted finite element methods. The main focus of this paper is the analysis and the treatment of the adverse effects of small cut elements.

3D Concrete Printing (3DCP) is an innovative construction technology that enables the efficient fabrication of complex objects through the extrusion of cementitious materials. However, the quality and integrity of the structural components are critically dependent on the accuracy of the extrusion and layer deposition processes. Study [8] employs the Particle Finite Element Method (PFEM) to virtually reproduce 3D printing of cementitious materials. PFEM allows for automatically tracking the free surface and efficiently modeling the material as a non-Newtonian Bingham fluid.

Flexoelectricity is a fundamental property found in all nano/micro-scale dielectric materials, even those with centrosymmetry. It describes coupling between the electric field and nonuniform mechanical strains, as well as between the electric field gradient and mechanical strains. Paper [9] presents a three-dimensional second-order collocation finite element method, which can model

higher-order electromechanical coupling and is computationally efficient. The formulations for the 27-noded mixed finite element based on the collocation principle are derived and translated into Fortran code.

An accurate simulation and computational analysis of temperature distribution in large power transformers used in power plants is crucial during both the design and operational phases. Paper [10] introduces a thermal modeling analysis encompassing two- and three-dimensional (2D and 3D) approaches for power transformers. The mathematical model for heat diffusion follows the Finite Element Method (FEM) approach.

Atomic force microscopy (AFM) is widely used to quantify mechanical properties, typically Young's modulus, by fitting force–indentation data with various mathematical contact models. Paper [11] focuses on the contact radius and Hertz-based extraction of Young's modulus.The results were compared to macroscopic data obtained using a standard measurement (ISO 527-1:2019) of Young's modulus. The contact was modeled using finite element analysis (FEA).

Paper [12**],** using the Finite Element Method, a solid model was created with images of femur bone tomography. Dynamic hip screws (DHS), cannulated screws (CCS), and medial buttress plates (MBP) were obtained by making three-dimensional designs. The required elements for the models were assigned, and the material properties of the elements were defined.

Research study [13] presents a comprehensive analysis of the local discontinuous Galerkin (LDG) method for solving multi-order fractional differential equations (FDEs), with an emphasis on circuit modeling applications. The results demonstrate that the LDG method achieves high-accuracy solutions (e.g., with a relatively large time step size) and reduced computational costs, which are attributed to its element-wise formulation.

Paper [14] presents a closed-loop control strategy for morphing wing structures where the feedback originates from monitoring the actual deformed shape of the morphed skin. The approach is based on the inverse Finite Element Method (iFEM), which is able to reconstruct the displacement field of a structure by minimizing, in a least-squares sense, the error between the analytical strains and those experimentally measured in some discrete locations. The iFEM-based control strategy is assessed numerically on the example problem of a wing segment whose trailing-edge camber is modified via the morphing strategy.

Paper [15] reveals the extension of a mathematical model of heat and mass transfer of fluid flow over a sheet by incorporating the effect of non-linear mixed convection. The governing equations of flow phenomena are expressed as partial differential equations (PDEs). Similarity transformations are employed to get a dimensionless set of boundary value problems. This study implements the finite element method to tackle the boundary value problems, based on the Galerkin approach.

Prof. Yu. K. Dem'yanovich of St. Petersburg State University focused on approximations over manifolds and, in particular, approximations on a sphere. The authors are grateful to Yu. K. Dem'yanovich for consultations and mentoring.

In this paper, we discuss the application of the Zlamal approximation to constructing an approximation on a sphere. As is known from mathematical analysis and geometry, a surface in space can be defined using various coordinate systems. One way to define a coordinate system is using Cartesian coordinates.

However, such a definition is only allowed for surfaces that project one-to-one onto one of the coordinate planes. Closed surfaces, such as a sphere, must be broken down into intersecting pieces. These pieces are called maps. The term "map" is used because the Earth's surface is a sphere; in cartography, the Earth's sphere is represented by a set of two-dimensional maps. A set of maps constitutes an atlas of the Earth's surface.

Here we consider a triangulation and atlas for a two-dimensional closed surface M, smoothly embedded in three-dimensional space. Suppose that the nodes (vertices) of a two-dimensional closed surface are given and the topology of a triangulation with these vertices is specified; that is, the triangles and vertices are numbered, and there is an incidence table that can be used to determine which nodes are vertices of each triangle. We can give an example of a triangulation on a sphere. First, consider the triangulation generated by the four vertices of an inscribed regular tetrahedron and segments of great circle arcs. We refine this triangulation by a factor of four, connecting the midpoints of the triangles' sides with great circle arc segments. We project the triangles on the sphere orthogonally onto the tangent plane.

The paper is organized as follows. The second section discusses the Courant and Zlamal approximations on a plane, and the third section discusses the Zlamal approximation on a sphere.

2 Problem Formulation

2.1 Construction of a Piecewise Linear Approximation

Let $\mathcal{T}'$ be a triangulation of the plane R^2 formed by finite triangles. Let ξ'_i, $i = 1,2,3$, be the vertices of triangle T' on the plane R^2. Denote by $\mathfrak{Z}'_j$ the union of closed triangles T', containing the vertex ξ'_j. To each vertex ξ'_j we associate a piecewise linear function $\Omega_j(\xi')$. This function must vanish outside $\mathfrak{Z}'_j$ and $\Omega_j(\xi'_j) = 1$.

Let us take $j = 1$ and write out the function $\Omega_1(\xi')$.

Let us introduce the notation for the Cartesian coordinates of the triangle's vertices: $\xi'_i = (x'_i, y'_i), i = 1,2,3$. Let us also denote $\xi' = (x', y')$.

Now we have

$$\Omega_1(\xi') = \det\begin{pmatrix} 1 & 1 & 1 \\ x' & x'_2 & x'_3 \\ y' & y'_2 & y'_3 \end{pmatrix} / \det\begin{pmatrix} 1 & 1 & 1 \\ x'_1 & x'_2 & x'_3 \\ y'_1 & y'_2 & y'_3 \end{pmatrix}, \quad (1)$$

Theorem 1. For function $U \in C^2(R^2)$ the approximation

$$\widetilde{U}(\xi') = \sum_j U(\xi'_j)\Omega_j(\xi') \quad (2)$$

gives the error of the approximation of the second order

$$\| U - \widetilde{U} \|_{C(R^2)} \leq Kh^2 \| U \|_{C^2(R^2)} \ . \quad (3)$$

Here h is the upper bound of the diameters of the triangles of the triangulation $\mathcal{T}'$.

Table 1 presents the errors of the Courant approximations for some functions at point (0.48, 0.5). The rows of this table correspond to the levels of grid refinement (n is the number of triangles in the triangulation).

Table 1. The errors of the Courant approximations for some functions at point (0.48, 0.5)

n	$\cos x^2$	$x^3 + y^3$	$\sin 5x + \cos 4y$	x^5
4^2	$2.3 \cdot 10^{-3}$	$-1.3 \cdot 10^{-2}$	$-4.1 \cdot 10^{-2}$	$-3.3 \cdot 10^{-3}$
4^3	$1.3 \cdot 10^{-3}$	$-6.6 \cdot 10^{-3}$	$-2.5 \cdot 10^{-2}$	$-2.0 \cdot 10^{-3}$
4^4	$5.6 \cdot 10^{-4}$	$-3.1 \cdot 10^{-3}$	$-1.2 \cdot 10^{-2}$	$-9.0 \cdot 10^{-4}$

Source: created by the authors.

2.2 Construction of the Zlamal Approximation

Now, we consider the Zlamal-type approximation on the plane.

Let us introduce the concept of barycentric coordinates. The barycentric coordinates of a point $\xi' \in R^2$ are the numbers $\lambda_1(\xi')$, $\lambda_2(\xi')$, and $\lambda_3(\xi')$ satisfying the equalities:

$\lambda_1(\xi') + \lambda_2(\xi') + \lambda_3(\xi') = 1,$
$\lambda_1(\xi')x'_1 + \lambda_2(\xi')x'_2 + \lambda_3(\xi')x'_3 = x',$
$\lambda_1(\xi')y'_1 + \lambda_2(\xi')y'_2 + \lambda_3(\xi')y'_3 = y'.$

Now we have

$$\lambda_1(\xi') = \det\begin{pmatrix} 1 & 1 & 1 \\ x' & x'_2 & x'_3 \\ y' & y'_2 & y'_3 \end{pmatrix} / \Delta, \quad (4)$$

$$\lambda_2(\xi') = \det\begin{pmatrix} 1 & 1 & 1 \\ x'_1 & x' & x'_3 \\ y'_1 & y' & y'_3 \end{pmatrix} / \Delta, \text{'} \quad (5)$$

$$\lambda_3(\xi') = \det\begin{pmatrix} 1 & 1 & 1 \\ x'_1 & x'_2 & x' \\ y'_1 & y'_2 & y' \end{pmatrix} / \Delta, \quad (6)$$

where

$$\Delta = \det\begin{pmatrix} 1 & 1 & 1 \\ x'_1 & x'_2 & x'_3 \\ y'_1 & y'_2 & y'_3 \end{pmatrix} \quad (7)$$

Properties of barycentric coordinates

1) $\lambda_j(\xi')$ is a first-degree polynomial, where $\lambda_j(\xi'_i) = \delta_{ij}$, $i, j = 1,2,3$;

2) The equation $\lambda_j(\xi') = 0$ defines the line on which the side of the triangle opposite the vertex ξ'_j is situated;

3) The interior points of the triangle are described by the system of inequalities

$$\lambda_i(\xi') > 0, \qquad i = 1,2,3;$$

4) The functions $\lambda_i(\xi')$ are not additive and homogeneous, but if the real numbers $\sigma>0$ and $\bar{\sigma}>0$ are such that $\sigma + \bar{\sigma} = 1$, then $\lambda_i(\sigma\,\xi' + \bar{\sigma}\,\bar{\xi}') = \lambda_i(\sigma\,\xi') + \lambda_i(\bar{\sigma}\,\bar{\xi}') = \sigma\,\lambda_i(\xi') + \bar{\sigma}\lambda_i(\bar{\xi}')$;

5) $\Omega_1(\xi') = \lambda_1(\xi')$.

We introduce the notation

$$J_0 = \{1,2,3\}, \quad \hat{\xi}'_{kl} = (\xi'_k + \xi'_l)/2, \quad k, l \in J_0, \ k < l.$$

Let function U be continuous on $\overline{T}'$, where $\overline{T}'$ is the closed T' triangle.

Lemma 1. A polynomial of the second degree

$$\widehat{U}\ (\xi') = \sum_{i\in J_0} \lambda_i(\xi')\ (2\,\lambda_i(\xi') - 1)U(\xi_i') + 4 \sum_{k<l,k,l\in J_0} \lambda_k(\xi')\lambda_l(\xi')U(\hat{\xi}_{kl}') \qquad (8)$$

interpolates the function U at the nodes ξ_i', $\hat{\xi}_{kl}'$.

Proof.
Substituting $\xi' = \xi_j'$ we obtain from (8)

$$\widehat{U}\ (\xi_j') = \sum_{i\in J_0} \lambda_i(\xi_j')\ (2\,\lambda_i(\xi_j') - 1)U(\xi_i') + 4 \sum_{k<l,k,l\in J_0} \lambda_k(\xi_j')\lambda_l(\xi_j')U(\hat{\xi}_{kl}').$$

Using $\lambda_j(\xi_i') = \delta_{ij},\ i,j = 1,2,3,$ (see property 1)), we obtain that

$$\sum_{i\in J_0} \lambda_i(\xi_j')\ (2\,\lambda_i(\xi_j') - 1)U(\xi_i') = U(\xi_j'),$$

because nonzero will be only that the term for which $i = j,$ and

$$\sum_{k<l,k,l\in J_0} \lambda_k(\xi_j')\lambda_l(\xi_j')U(\hat{\xi}_{kl}') = 0,$$

because every the term is zero.

Thus, we have the relation:

$$\widehat{U}\ (\xi_j') = U(\xi_j').$$

Substituting $\xi' = \xi_{st}',\ s,t \in J_0,\ s < t,$ then we have

$$\widehat{U}\ (\xi_{st}') = \sum_{i\in J_0} \lambda_i(\xi_{st}')\ (2\,\lambda_i(\xi_{st}') - 1)U(\xi_{st}') + 4 \sum_{k<l,k,l\in J_0} \lambda_k(\xi_{st}')\lambda_l(\xi_{st}')U(\hat{\xi}_{kl}').$$

when $\sigma = \bar{\sigma} = \frac{1}{2},\ \xi' = \xi_s', \bar{\xi}' = \xi_t',$ then

$$\lambda_i(\xi_{st}') = \frac{1}{2}(\delta_{is} + \delta_{it}),$$

where

$$\delta_{is} = \lambda_i(\xi_s'), \delta_{it} = \lambda_i(\xi_t').$$

Now we have

$$\widehat{U}\ (\xi_{st}') = \frac{1}{2}\sum_{i\in J_0} (\delta_{is} + \delta_{it})\ (\delta_{is} + \delta_{it} - 1)U(\xi_{st}') + 4 \sum_{k<l,k,l\in J_0} (\delta_{ks} + \delta_{kt})(\delta_{ls} + \delta_{lt})U(\hat{\xi}_{kl}').$$

In the first sum, the term is certainly zero if $i \neq s, i \neq t$. For $i = s, i = t,$ the terms are also zero. It is easy to show that in the second sum, if $s = 1, t = 2,$ then $\widehat{U}(\hat{\xi}_{12}') = U(\hat{\xi}_{12}')$. Similarly, for $s < t,$ we obtain the equality $\widehat{U}\ (\hat{\xi}_{st}') = U(\hat{\xi}_{st}')$.
Thus, the interpolation properties of the polynomial $\widehat{U}\ (\xi')$ are proven.

Assume that $U \in C^3(R^2)$. On each triangle T', consider a polynomial of degree two:

$$\widehat{U}\ (\xi') = \sum_{i\in J(T')} \lambda_i^{T'}(\xi')\ \left(2\,\lambda_i^{T'}(\xi') - 1\right)U(\xi_i') + 4 \sum_{k<l,k,l\in J(T')} \lambda_k^{T'}(\xi')\lambda_l^{T'}(\xi')U(\hat{\xi}_{kl}'). \quad (9)$$

Here $J(T')$ is the set of indices that number the vertices of the triangle T', $\lambda_j^{T'}(\xi')$ are the barycentric coordinates of the point ξ', determined by the vertices of $\overline{T}'$, $\overline{T}'$ is the closure T', $\hat{\xi}_{kl}' = (\xi_k' + \xi_l')/2,\ k, l \in J,\ k < l.$
Let T' and $T_1{}'$ be two adjacent triangles, and if the point ξ' lies on their common side, then it can be proved that the relation:

Lemma 2. $\widehat{U}^{T'}(\xi') = \widehat{U}^{T_1{}'}(\xi'),\ \xi' \in \overline{T'} \cap \overline{T'}_1.$

Proof. The proof is obvious, because, for the three points (the two ends and the middle point), the relation is valid. If we put $\xi' = \xi'(s),$ where s is the parameter that defines the length of the side, we can see that $\widehat{U}^{T'}(\xi'(s))$ and $\widehat{U}^{T_1{}'}(\xi'(s))$ are the polynomials of the second-degree, coinciding at three points, therefore, they coincide for all s under consideration.

On R^2, we define the function $\widehat{U}\ (\xi')$ by the equality $\widehat{U}\ (\xi') = \widehat{U}^{T'}(\xi')$, where $\xi' \in T', T'$ is any triangle in $\mathcal{T}'$.

The function $\widehat{U}\ (\xi')$ is called the Zlamal finite element approximation.

Theorem 2 The Zlamal approximation $\widehat{U}\ (\xi')$, defined by formulas (8) and (9), interpolates the function U at the points ξ_j' and $\hat{\xi}_{ij}'$:

$$\widehat{U}(\xi_j') = U\ (\xi_j'), \qquad \widehat{U}(\hat{\xi}_{ij}') = U\ (\hat{\xi}_{ij}').$$

The proof follows from *Lemma 2.*

Corollary The Zlamal approximation is exact on second-degree polynomials

$$\widehat{U}\ (\xi') = U(\xi'),\ \xi' \in R^2.$$

Proof. From the statement of Theorem 1 and formula (9), it follows that the second-degree polynomial

$$P(\xi') = \sum_{i\in J(T')} \lambda_i^{T'}(\xi')\left(2\,\lambda_i^{T'}(\xi') - 1\right)V_i + 4 \sum_{k<l,k,l\in J(T')} \lambda_k^{T'}(\xi')\lambda_l^{T'}(\xi')V_{kl}\ ,\xi' \in \overline{T'} \quad (10)$$

gives a solution to the interpolation problem

$$P\left(\xi_j'\right) = V_j,\ j \in J(T'),$$
$$P\left(\xi_{m,n}'\right) = V_{m,n},\ m < n,\ m,n \in J(T'),$$

in the class of second-degree polynomials π_2 in two variables. Formula (10) can be viewed as a linear mapping of the six-dimensional space of coefficients $V_j, V_{m,n}$ into the six-dimensional space π_2.The kernel of this mapping consists of a single zero. Therefore, mapping (10) maps the space π_2 onto itself. To obtain a polynomial $P \in \pi_2$ in formula (10), we must set $V_j = P\left(\xi_j'\right)$, $V_{kl} = P(\xi_{kl}')$. Thus, mapping (10) is the identity transformation on the space π_2.
The corollary is proved.

Table 2 presents the errors of the Zlamal approximations for some functions at point (0.48, 0.5). The rows of this table correspond to the levels of grid refinement (n is the number of triangles in the triangulation).

Table 2. The errors of the Zlamal approximations for some functions at point (0.48, 0.5)

n	$\cos x^2$	$x^3 + y^3$	sin 5x + cos 4y	x^5
4^2	$3.7 \cdot 10^{-4}$	$-4.8 \cdot 10^{-4}$	$-9.8 \cdot 10^{-3}$	$-7.9 \cdot 10^{-4}$
4^3	$7.6 \cdot 10^{-5}$	$-8.9 \cdot 10^{-5}$	$-1.6 \cdot 10^{-3}$	$-1.8 \cdot 10^{-4}$
4^4	$8.5 \cdot 10^{-6}$	$-9.6 \cdot 10^{-6}$	$-1.5 \cdot 10^{-4}$	$-2.1 \cdot 10^{-5}$

Source: created by the authors

2.3 A Generalization of the Zlamal Approximation on the Plane

Now let us consider a generalization of the Zlamal approximation.
Let σ_{ij} and σ_{ji} be numbers such that
$\sigma_{ij} + \sigma_{ji} = 1$, $\sigma_{ij}, \sigma_{ji} \in (0,1)$, $i<j$, $i,j \in J(T')$.
Consider the points $\xi_{ij}' = \sigma_{ij}\xi_i' + \sigma_{ji}\xi_j'$.

By virtue of property 4) of the previous section

$$\lambda_i\left(\sigma\,\xi' + \bar{\sigma}\,\bar{\xi}'\right) = \lambda_i(\sigma\xi') + \lambda_i\left(\bar{\sigma}\,\bar{\xi}'\right)$$

we obtain

$$\lambda_i^{T'}(\xi_{kl}') = \sigma_{kl}\lambda_i^{T'}(\xi_k') + \sigma_{lk}\lambda_i^{T'}(\xi_l').$$

By virtue of property 1), $\lambda_j(\xi')$ is a first-degree polynomial, and $\lambda_j(\xi_i') = \delta_{ji}$, $i,j = 1,2,3$, we obtain for $i \neq k, i \neq l$ the following relations $\lambda_i^{T'}(\xi_{il}') = \sigma_{il}$, $\lambda_i^{T'}(\xi_{ki}') = \sigma_{ik}$, $\lambda_i^{T'}(\xi_{kl}') = 0$.

On functions $u \in C(R^2)$, we introduce the operator A by the equality $\widetilde{U}^{T'}(\xi') = AU$, where

$$\widetilde{U}^{T'}(\xi') = \sum_{i\in J(T')} \lambda_i^{T'}(\xi')\left(\left(\lambda_j^{T'}(\xi') - 1\right)q_i/2 + U(\xi_i')\right) + \sum_{i<j,i,j\in J(T')} \lambda_i^{T'}(\xi')\,\lambda_j^{T'}(\xi')\,U(\xi_{ij}')/(\sigma_{ij}\,\sigma_{ji})\,,$$
$$\xi' \in T', \quad (11)$$

here

$$q_1 = U(\xi_1')(\sigma_{21}^{-1} + \sigma_{31}^{-1}) + U(\xi_2')(\sigma_{12}^{-1} - \sigma_{32}^{-1}) + U(\xi_3')(\sigma_{13}^{-1} - \sigma_{23}^{-1}),$$
$$q_2 = U(\xi_1')(\sigma_{21}^{-1} - \sigma_{31}^{-1}) + U(\xi_2')(\sigma_{12}^{-1} + \sigma_{32}^{-1}) + U(\xi_3')(\sigma_{23}^{-1} - \sigma_{13}^{-1}),$$
$$q_3 = U(\xi_1')(\sigma_{31}^{-1} - \sigma_{21}^{-1}) + U(\xi_2')(\sigma_{32}^{-1} - \sigma_{12}^{-1}) + U(\xi_3')(\sigma_{13}^{-1} + \sigma_{23}^{-1}).$$

We assume that ξ_1', ξ_2', ξ_3' are the vertices. Therefore, we can take $J(T') = \{1,2,3\}$. It is easy to establish the interpolation properties of the mapping A: $\widetilde{U}^{T'}(\xi_{kl}') = U(\xi_{kl}')$, $k<l$, $k, l=1,2,3$.

Lemma 3 (Dem'yanovich). $\widetilde{U}^{T'}(\xi_{kl}') = U(\xi_{kl}')$, $k < l, k, l = 1,2,3$.

Denote $a = \sigma_{21}^{-1}, b = \sigma_{31}^{-1}, c = \sigma_{32}^{-1}, a' = \sigma_{12}^{-1}, b' = \sigma_{13}^{-1}, c' = \sigma_{23}^{-1}$.
We have

$$(AU)(\xi') = \lambda_1(\xi')((\lambda_1(\xi') - 1)q_1/2 + U(\xi_1')) + \lambda_2(\xi')(\tfrac{(\lambda_2(\xi')-1)q_2}{2} + U(\xi_2')) + \lambda_3(\xi')((\lambda_3(\xi') - 1)q_3/2 + U(\xi_3')) + \lambda_1(\xi')\lambda_2(\xi')\,a\,a'U(\xi_{12}') + \lambda_1(\xi')\lambda_3(\xi')\,b\,b'U(\xi_{13}') + \lambda_2(\xi')\lambda_3(\xi')\,c\,c'U(\xi_{23}'),$$

$$q_1 = U(\xi_1')(a + b) + U(\xi_2')(a' - c) + U(\xi_3')(b' - c'),$$
$$q_2 = U(\xi_1')(a - b) + U(\xi_2')(a' + c) + U(\xi_3')(c' - b'),$$
$$q_3 = U(\xi_1')(b - a) + U(\xi_2')(c - a') + U(\xi_3')(b' + c'),$$

Note. When $\sigma_{ij} = \frac{1}{2}$, then $a = a' = b = b' = c = c' = 2, q_i = 4U(\xi_i')$.
We denote

$$S_1(\xi') = \sum_{i\in\{1,2,3\}} \lambda_i(\xi')((\lambda_i(\xi')-1)q_i/2 + U(\xi_i')),$$

$$S_2(\xi') = \sum_{i<j,i,j=1,2,3} \lambda_i(\xi')\lambda_j(\xi')\, U(\xi_{ij}')/(\sigma_{ij}\,\sigma_{ji}),$$

Obviously we have

$$S_1(\xi_k') = U(\xi_k'), \quad S_2(\xi_k') = 0,$$

thus

$$\widetilde{U}(\xi_k') = U(\xi_k'), k = 1,2,3,$$

and

$$S_1(\xi_{kl}') = \lambda_k(\xi_{kl}')(\frac{(\lambda_k(\xi_{kl}')-1)q_k}{2} + U(\xi_k')) + \lambda_l(\xi_{kl}')\left(\frac{(\lambda_l(\xi_{kl}')-1)q_l}{2} + U(\xi_l')\right).$$

We can rewrite this formula in the following form:

$$S_1(\xi_{kl}') = \sigma_{kl}\left(\frac{(\sigma_{kl}-1)q_k}{2} + U(\xi_k')\right) + \sigma_{lk}\left(\frac{(\sigma_{lk}-1)q_l}{2} + U(\xi_l')\right) = -\frac{\sigma_{kl}(1-\sigma_{kl})(q_k+q_l)}{2} + \sigma_{kl}\,U(\xi_k') + (1-\sigma_{kl})U(\xi_l').$$

We can take $k = 1, l = 2$. In this case, we have

$$q_1 + q_2 = 2\frac{U(\xi_1')}{\sigma_{21}} + 2\frac{U(\xi_2')}{\sigma_{12}}.$$

Thus

$$S_1(\xi_{12}') = -\sigma_{12}\,\sigma_{21}\left(\frac{U(\xi_1')}{\sigma_{21}} + \frac{U(\xi_2')}{\sigma_{12}}\right) + \sigma_{12}\,U(\xi_1') + \sigma_{12}\,U(\xi_2') = 0.$$

Similary, we have

$$S_1(\xi_{13}') = S_1(\xi_{23}') = 0.$$

So $S_1(\xi_{kl}') = 0$.

And we can obtain the relation:

$$S_2(\xi_{kl}') = \frac{\lambda_1(\xi_{kl}')\lambda_2(\xi_{kl}')}{\sigma_{kl}\,\sigma_{lk}}U(\xi_{kl}') = U(\xi_{kl}').$$

Finally we obtain

$$\widetilde{U}^{T'}(\xi_{kl}') = U(\xi_{kl}'), k < l, k, l = 1,2,3.$$

Lemma 4. Relation (11) defines an interpolation polynomial of degree two with interpolation nodes ξ_i', ξ_{ij}', where ξ_i', ξ_{ij}', such that

$$\xi_{ij}' = \sigma_{ij}\xi_i' + \sigma_{ji}\xi_j',\ i<j,\ i,j \in J(T').$$

The operator A is the identity operator on the set of polynomials of degree two.

For a function $U \in C^3(R^2)$, on each triangle T' of a triangulation $\mathcal{T}'$, consider the polynomial $\widetilde{U}^{T'}(\xi'), \xi' \in T'$. We define the function $\widetilde{U}(\xi'), \xi' \in R^2$, by the equality

$$\widetilde{U}(\xi') = \widetilde{U}^{T'}(\xi'),\ \xi' \in T',\ T' \in \mathcal{T}'. \quad (12)$$

The function $\widetilde{U}(\xi')$ generalizes the Zlamal finite element approximation.

Theorem 3. The approximation $\widetilde{U}(\xi')$, satisfying relations (11), (12), is continuous on the entire plane and interpolates the function at the points ξ_j', ξ_{ij}'

$$\widetilde{U}(\xi_j') = U(\xi_j'), \quad \widetilde{U}(\xi_{ij}') = U(\xi_{ij}'),$$

The proof is easy to obtain using *Lemma 4.*

It is convenient to represent the approximation $\widetilde{U}(\xi')$ in the form:

$$\widetilde{U}(\xi') = \sum_k U(\xi_k')\,\Omega_k(\xi') + \sum_{i<j} U(\xi_{ij}')\,\Omega_{ij}(\xi'),$$

where

$$\xi_{ij}' = \sigma_{ij}\xi_i' + \sigma_{ji}\xi_j',\ i<j,$$
$$\sigma_{ij} + \sigma_{ji} = 1, \sigma_{ij}, \sigma_{ji} \in (0,1),$$

$$\Omega_k(\xi') = \begin{cases} \frac{\lambda_k^{T'}(1-\lambda_i^{T'})}{\sigma_{ik}} - \frac{\lambda_j^{T'}}{\sigma_{jk}},\ \xi' \in T', T' \subset \mathfrak{Z}_k' \\ 0,\ \xi' \notin \mathfrak{Z}_k' \end{cases} \quad (13)$$

$$\Omega_{kl}(\xi') = \begin{cases} \frac{\lambda_k^{T'}\lambda_l^{T'}}{\sigma_{kl}\sigma_{lk}},\ \xi' \in T',\ T' \subset \mathfrak{Z}_k' \cap \mathfrak{Z}_l' \\ 0,\ \xi' \notin \mathfrak{Z}_k' \cap \mathfrak{Z}_l' \end{cases}, \quad (14)$$

Recall that $\mathfrak{Z}_k'$ is the union of closed triangles from $\mathcal{T}'$, and $\mathfrak{Z}_{kl}'$ is the union of closed triangles containing the vertices ξ_k' and ξ_l'. Obviously, supp $\Omega_{kl} = \mathfrak{Z}_{kl}'$ (Figure 1), and supp $\Omega_k = \mathfrak{Z}_k'$ (**Figure 2**).

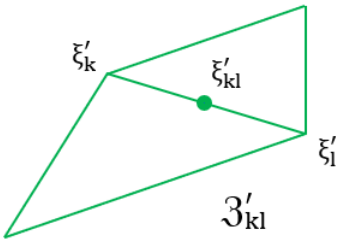


Fig. 1: $\mathfrak{Z}_{kl}'$ is the union of closed triangles containing the vertices ξ_k' and ξ_l'.
Source: created by the authors.

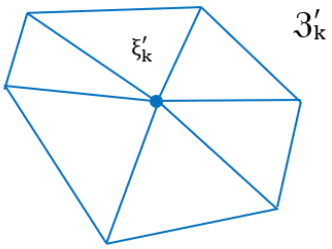


Fig. 2: supp $\Omega_k = 3'_k$
Source: created by the authors.

Remark. We do not indicate the dependence of $\lambda_j^{T'}$ from ξ' .

The following statements hold:
$\Omega_k(\xi'_k) = 1; \Omega_k(\xi'_i) = 0$, if $k \neq i$;
$\Omega_{ij}(\xi'_{ij}) = 1; \Omega_{ij}(\xi'_{kl}) = 0$, if $k \neq i,\ j \neq l$;
$\Omega_k(\xi'_{ij}) = 0,\ k < l;\ \Omega_{ij}(\xi'_k) = 0.$

Theorem 4. For functions $U \in C^3(R^2)$ the approximation

$$\widetilde{U}(\xi') = \sum_k U(\xi'_k)\,\Omega_k(\xi') + \sum_{i<j} U(\xi'_{ij})\,\Omega_{ij}(\xi'),$$
$$\xi'_{ij} = \sigma_{ij}\xi'_i + \sigma_{ji}\xi'_j\ ,\ i<j,\ ,\sigma_{ij} + \sigma_{ji} = 1,$$
$$\sigma_{ij}, \sigma_{ji} \in (0,1),$$

gives the error of the approximation of the third order

$$\| U - \widetilde{U} \|_{C(R^2)} \leq Kh^3 \| U \|_{C^3(R^2)}.$$

Here h is the upper bound of the diameters of the triangles of the triangulation T' and the constant K is independent of h.

The proof is based on the fact that the approximation $\widetilde{U}$ is exact on second-degree polynomials and the application of Taylor's formula.

Remark. In practical calculations, it is necessary to ensure that the quantities σ_{ij}, σ_{ji} are not too small; otherwise, the process may become unstable.

For example. If we approximate the function $3x(x-1)$ in the triangle (Figure 3) with the program developed in C with float-type numbers when eps=0.0001, we obtain the approximation with error=0.0, but when eps=0.00001 we obtain the approximation with error=0.021.

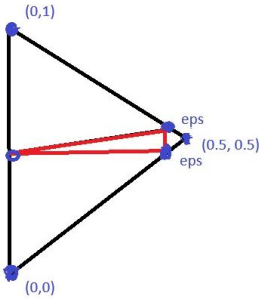


Fig. 3: The triangle with small eps.
Source: created by the authors

If we approximate the function $3x(x-1)$ with the program developed in C with double-type numbers when eps=0.0001 we obtain the approximation with error=0, but when eps=0.00001 we obtain the approximation with error=5.8 10^{-11}.

Table 3 presents the errors of approximation with generalization of the Zlamal functions ($\sigma_{ij} = 1/3$) at point (0.49, 0.5). The rows of this table correspond to the levels of grid refinement (n is the number of triangles in the triangulation).

Table 3. The errors of approximation with generalization of the Zlamal functions ($\sigma_{ij} = 1/3$) at point (0.49, 0.5)

n	$\cos x^2$	$x^3 + y^3$	$\sin 5x + \cos 4y$
4^2	$2.7 \cdot 10^{-4}$	$-5.0 \cdot 10^{-4}$	$-5.5 \cdot 10^{-3}$
4^3	$1.2 \cdot 10^{-4}$	$1.5 \cdot 10^{-5}$	$-1.5 \cdot 10^{-3}$
4^4	$5.0 \cdot 10^{-4}$	$1.4 \cdot 10^{-5}$	$-4.1 \cdot 10^{-4}$

Source: created by the authors.

Table 4 presents the errors of approximation with generalization of the Zlamal functions ($\sigma_{ij} = 1/4$) at point (0.49, 0.5). The rows of this table correspond to the levels of grid refinement (n is the number of triangles in the triangulation).

Table 4. The errors of approximation with generalization of the Zlamal functions ($\sigma_{ij} = 1/4$) at point (0.49, 0.5)

n	$\cos x^2$	$x^3 + y^3$	$\sin 5x + \cos 4y$
4^2	$3.3 \cdot 10^{-4}$	$9.9 \cdot 10^{-6}$	$-7.3 \cdot 10^{-3}$
4^3	$2.0 \cdot 10^{-4}$	$3.0 \cdot 10^{-5}$	$-3.3 \cdot 10^{-3}$
4^4	$1.1 \cdot 10^{-4}$	$2.3 \cdot 10^{-5}$	$-1.4 \cdot 10^{-3}$

Source: created by the authors.

Comparison of the results of applying the Courant (Table 1) and Zlamal functions firstly highlights the advantage of using the Zlamal functions, and secondly confirms the theoretical estimates of the approximation.

3 The Zlamal-type Approximation on a Sphere

Let us now construct the coordinate functions on a sphere M in the space R^3 with the center at 0:

$$(\xi,\xi)=r^2.$$

We assume that the sphere is triangulated in the same way as in [16]. Besides the vertices ξ_j of the triangulation $\mathcal{T}$, $i\in J$, for a pair of vertices ξ_k, ξ_l of each triangle $T\in\mathcal{T}$, $k<l$, take a point $\xi_{kl}=(\xi_k+\xi_l)\times\| \xi_k+\xi_l \|^{-1}$ on M.

Putting $U_\zeta=\{\xi \mid (\xi,\zeta)\geq \varepsilon r^2\}$ $(\varepsilon\in(0,1), \varepsilon=$ const) we consider the mapping [16]

$$\chi_\zeta: \xi\longrightarrow \xi', \quad \xi'=\tau\xi-\zeta, \quad (15)$$

where $\tau=\frac{r^2}{(\xi,\zeta)}$.

For points ξ_i, ξ_{kl} which are in $\overline{T}$, we consider the points

$\xi_i'=\chi_\zeta(\xi_i)$, $\xi_{kl}'=\chi_\zeta(\xi_{kl})$, $k<l$, $i,k,l\in J$

on the plane L_ζ. The images ξ_i' of the vertices ξ_i of triangle $\overline{T}$ obviously are not situated on one straight line; we connect them by the straight line segments in L_ζ and denote the resulting triangle by T'.

Obviously, $0\in T'$. In the triangle $\overline{T'}$ we construct the functions $\Omega_i^Z(\xi')$ and $\Omega_{kl}^Z(\xi')$ using formulas (13) and (14); due to the dependence of the points ξ_i' and ξ_{kl}' on $\zeta\in$ M, these functions depend on ζ. In what follows, we will denote them by $\omega_{\zeta,i}^Z(\xi')$ and $\omega_{\zeta,kl}^Z(\xi')$, respectively.

In view of the relation $\xi_{kl}'=\sigma_{kl}\xi_k'+\sigma_{lk}\xi_l'$, the quantities σ_{kl} in formulas (13) and (14) depend on ζ, namely,

$$\sigma_{ij}=(\zeta,\xi_i)/(\zeta,\xi_i+\xi_j), \quad i,j\in J. \quad (16)$$

Since we need the values $\omega_{\zeta,i}^Z(0)$ and $\omega_{\zeta,kl}^Z(0)$, then, as can be seen from (13) and (14), it is required to find the barycentric coordinates of the point 0 in the triangle T' depending on the variable $\zeta\in$ M. Considering that the vertices of the corresponding triangle T $\in\mathcal{T}$ are the points ξ_1, ξ_2, and ξ_3, we have

$$\lambda_i(0)=(\zeta,\xi_i)\Delta_i^T/(r^2\,\Delta^T) \quad (17)$$

where Δ^T is the third-order determinant whose columns are the vectors ξ_1, ξ_2, and ξ_3, and where Δ_i^T is the determinant obtained from Δ^T by replacing the i-th column with the vector ζ.

From basis functions of Courant approximations on the sphere, and formulas (13) through (17), we find the basis functions of the Zlamal approximation on the sphere, which have the form:

$$\omega_i^z(\zeta)=\begin{cases}\frac{(\xi_i,\zeta)^2\Delta_i^T(\zeta)}{r^4(\Delta^T)^2}(\Delta_i^T(\zeta)-\sum_{j,j\neq i}\Delta_j^T(\zeta)), \xi_i,\zeta\in\overline{T}\\ 0, \text{otherwise}\end{cases}$$

$$\omega_{kl}^z(\zeta)=\begin{cases}(\xi_k+\xi_l,\zeta)^2\Delta_k^T(\zeta)\Delta_l^T(\zeta)/(r^4(\Delta^T)^2), \xi_l,\xi_i,\zeta\in\overline{T}\\ 0, \text{otherwise}\end{cases}$$

As well as plane Zlamal functions, the functions above are continuous and satisfy the following interpolation relations

$$\omega_i^z(\xi_j)=\delta_{i,j},\ \omega_{kl}^z(\xi_{k'l'})=\delta_{k,k'}\delta_{l,l'},$$
$$\omega_{kl}^z(\xi_j)=0,\ \omega_i^z(\xi_{kl})=0,$$

where $k<l, k'<l'$ and $i,j,k,l,k',l'\in J$.

The support of the function ω_i^z is the closure of the barycentric star with the vertex ξ_i, and the support of the function ω_{kl}^z is the union of two closed triangles whose vertices are the points ξ_k and ξ_l, where $k<l$.

Note that, due to the properties of basis splines and the interpolation relations, the approximation

$$\widetilde{U}(\zeta)=\sum_i U(\xi_i)\,\omega_i^z(\zeta)+\sum_{k<l}U(\xi_{kl})\,\omega_{kl}^z(\zeta),$$

is continuous, exact on second-degree polynomials, and approximates the function $U\in C^3(M)$ with order h^3 in the $C(M)$ metric, where

$$h=\max_{T\in\mathcal{T},\xi_i,\xi_j\in\overline{T}}\|\xi_i-\xi_j\|.$$

The proof is based on the fact that the approximation $\widetilde{U}(\zeta)$ is exact on second-degree polynomials and the application of Taylor's formula.

Table 5 presents the errors of the Courant approximations on a sphere for some functions $f(x,y,z)$ at point $\zeta_{1,3}$ with angular coordinates

$$(-\tfrac{3\pi}{10}, \tfrac{6\pi}{5}).$$

Table 5. The errors of the Courant approximations on a sphere for some functions $f(x,y,z)$ at point $\zeta_{1,3}$ with angular coordinates $(-\frac{3\pi}{10}, \frac{6\pi}{5})$

n	$\cos x^2$	x^3+y^3	$\exp(z-y^2)$	x^5
$2\,4^2$	-1.2 10^{-3}	3.2 10^{-2}	3.510^{-3}	2.1 10^{-2}
$2\,4^3$	7.1 10^{-4}	1.5 10^{-2}	1.0 10^{-3}	7.5 10^{-3}
$2\,4^4$	2.2 10^{-4}	3.7 10^{-3}	1.4 10^{-4}	1.4 10^{-3}

Source: created by the authors.

Next, we recall some auxiliary statements.

Let M be some n-dimensional manifold (i.e., a topological space in which every point has a neighborhood homeomorphic to an n-dimensional ball in the Euclidean space R^{n+1}), let E_ζ be an open ball in the space R^{n+1}, let Z be some set of indices, and let there be a system of differentiable coordinates on the manifold M$\in C^k$, i.e., a family of open sets $\{U_\zeta\}_{\zeta\in Z}$ covering M, and homeomorphisms ψ_ζ, $\psi_\zeta: E_\zeta \to U_\zeta$ such that the mappings

$$\psi_\zeta^{-1}\,\psi_{\zeta'}:\ \psi_{\zeta'}^{-1}\left(U_\zeta\cap U_{\zeta'}\right)\to \psi_\zeta^{-1}(U_\zeta\cap U_{\zeta'}),\quad \zeta,\zeta'\in Z \quad (18)$$

are continuously differentiable. Here $\psi_\zeta: E_\zeta \to U_\zeta$ is called a map and the set $\{\psi_\zeta: E_\zeta \to U_\zeta \mid \zeta\in Z\}$ is called an atlas. Next we take n=2.

Definition. A function u is said to be defined on a manifold M, if for each $\zeta\in Z$, a function $F_\zeta(x)$ $\left(x\in E_\zeta\right)$ is defined such that the relations $F_\zeta\left(x_\zeta\right)=F_{\zeta'}\left(x_{\zeta'}\right)$, $x_\zeta=\psi_\zeta^{-1}(\xi)$, $x_{\zeta'}=\psi_{\zeta'}^{-1}(\xi)$, $\xi\in U_\zeta\cap U_{\zeta'}$ are valid.

Let function $U\in C^3$(M) be defined on a manifold M. By definition, this means that functions $F_\zeta\in C^3\left(E_\zeta\right)$, $\zeta\in$ M, are given, and with these functions F_ζ the function $U=F_\zeta\circ\psi^{-1}$ is uniquely determined.

Let $f(\eta)$ be an abstract function with values in the space $(\mathrm{C}^3(\mathrm{M}))^*$, $\eta\in$ M; let the support of the functional $f(\eta)$ (for a fixed η) lie in the set U_η.

Theorem 5 (Demyanovich). If $f(\zeta)$ is a continuous abstract function on a compact manifold M with values in C*(M), then the following estimate holds:

$$\|U-\widetilde{U}\|_{\mathrm{C(M)}}\le C_0K_0h^3\,\|U\|_{\breve{\mathrm{C}}^3(\mathrm{M})},$$

where the constant C_0 is independent of ζ and F_ζ, $K_0=\sup\limits_{\zeta\in\mathrm{M}}\|f(\zeta)\|_{\mathrm{C}^*(\mathrm{M})}$, $h=\sup\limits_{\zeta\in\mathrm{M}}h(\zeta)$, and

$$\|U\|_{\breve{C}^k(\mathrm{M})}=\sup_{\zeta\in\mathrm{M}}\|F_\zeta\|_{\mathrm{C}^k(\mathrm{E}_\zeta)},\quad (19)$$

$$S(\zeta)=\operatorname{supp} f(\zeta),\qquad S'(\zeta)=\psi_\zeta^{-1}\left(S(\zeta)\right),$$
$$h(\zeta)=\operatorname{diam} S'(\zeta).$$

Proof is given in [17].

Next, we give the notion of an admissible atlas on a compact manifold. Recall that an atlas $A=\{\mathcal{X}_i:\ E_i\to M_i\mid i=1,\dots,i_0\}$ is said to be admissible for a differentiable manifold of class C^k if homeomorphisms

$$\mathcal{X}_i^{-1}\,\mathcal{X}_{i'}:\ \mathcal{X}_{i'}^{-1}\quad \mathcal{X}_i^{-1}\,(\mathrm{M}_i\cap\mathrm{M}_{i'}) \quad (20)$$

are k times continuously differentiable. In what follows, we assume that E_i and E_ζ are open balls in R^n centered at the origin.

An atlas $\widetilde{\boldsymbol{A}}$ consisting of some maps of an atlas $\boldsymbol{A}$ is called a sub-atlas of $\boldsymbol{A}$; we write $\tilde{A}\subset A$. Functions $\Phi_i(\xi')$, $i=1,\dots,i_0$, are said to represent a function $u(\zeta)$, $\zeta\in$ M, in the atlas A, if

$$u(\zeta)=\Phi\left(\mathcal{X}_i^{-1}\zeta\right),\qquad \zeta\in\mathrm{M_i}.$$

We show that, under certain conditions, the norm $\|u\|_{\breve{C}(\mathrm{M})}$ is equivalent to the commonly accepted norm defined as follows.

Let M$\in C^k$, let $A=\{\mathcal{X}_i:\ E_i\to M_i\mid i=1,\dots,i_0\}$ be an admissible atlas, and the function $U(\zeta)$, $\zeta\in$ M, is represented by the functions Φ_i in the atlas A. We shall say that u lies in the space $\hat{C}^k$(M) of the norm

$$\|U\|_{\hat{C}^k(M)}=\max_{i=1,\dots,i_0}\|\Phi_i\|_{C^k(\bar{E}_i)} \quad (21)$$

is defined and finite.

It is easy to see that the space $\hat{C}^k(M)$ is Banach, its elementwise composition does not depend on the choice of admissible atlas, and although the norms (21) depend on such a choice, for two admissible atlases these norms are equivalent.

In the end, we introduce the following condition:

Condition (B). On the manifold M there exists an admissible atlas $A=\{\mathcal{X}_i:\ E_i\to\mathrm{M}_i\mid i=1,\dots,i_0\}$ and a finite cover $\{\mathrm{M}_i\mid i=1,\dots,i_0\}$ by open sets M_i such that, for every $i\in\{1,\dots,i_0\}$, the mappings

$$\mathcal{X}_i^{-1}\,\psi_\zeta:\ E_\zeta\cap\psi_\zeta^{-1}\mathcal{X}_{\,i}\,E_i\to\ \mathcal{X}_i^{-1}\psi_\zeta\,E_\zeta\cap E_i,$$

are k times continuously differentiable and their derivatives are uniformly bounded with respect to the parameter $\zeta\in\mathrm{M}_i$. Moreover, it is assumed that if $A=\{U_{\zeta_i}\mid i=1,\dots,i_0\}$ is a finite cover of the manifold M, then there corresponds to it an admissible atlas

$$U=\{\psi_{\zeta_i}:E_{\zeta_i}\to U_{\zeta_i}\mid i=1,\dots,i_0\}.$$

Remark. If M is an n-dimensional manifold of class C^{k+2} smoothly embedded in R^{n+1}, and if $\{\psi_i^{-1}\}$ is a family of orthogonal projections onto the tangent plane L_ζ drawn to M at the point ζ, then condition (B) is satisfied.

Theorem 6 *If condition (B) holds for a compact manifold M of class* C^{k+1}, *then norms* (19) *and* (21) *are equivalent.*

The proof can be found in [17].

Theorem 7 The Zlamal-type approximation

$$\tilde{U}(\xi) = \sum_{i \in J} U(\xi_i)\, \omega_i^Z(\xi) + \sum_{k<l,k,l \in J} U(\xi_{kl})\, \omega_{kl}^Z(\xi)$$

approximates the function U with the order h^3 in the metric $\mathrm{C(M)}$, where

$$h = \max_{T \in \mathcal{T}} \max_{\xi_i, \xi_j \in \overline{\mathrm{T}}} ||\xi_i - \xi_j||.$$

The proof of the theorem follows from the construction of the functions ω_i^Z and ω_{kl}^Z, and from Theorems 5 and 6, which are stated above.

Table 6 presents the errors of the Zlamal approximations on a sphere for the function $f(x,y,z) = x$ defined on the unit sphere at points ζ_{ki} with angular coordinates $(\frac{k\pi}{4} - \frac{\pi}{2}, \frac{\pi i}{2})$.

Table 6. Errors in the Zlamal-type approximation of the function $f(x,y,z) = x$ defined on the unit sphere at points ζ_{ki} with angular coordinates $(\frac{k\pi}{4} - \frac{\pi}{2}, \frac{\pi i}{2})$

n	$\zeta_{1,1}$	$\zeta_{1,2}$	$\zeta_{1,3}$	$\zeta_{1,4}$
4^2	$8.7\ 10^{-3}$	$2.7\ 10^{-2}$	$-1.2\ 10^{-3}$	$-2.8\ 10^{-2}$
4^3	0	$3.6\ 10^{-4}$	$-3.2\ 10^{-3}$	$-9.8\ 10^{-3}$
4^4	0	$4.3\ 10^{-4}$	$-6.7\ 10^{-4}$	$-1.3\ 10^{-3}$
4^5	0	$5.4\ 10^{-5}$	$-2.7\ 10^{-5}$	$-2.5\ 10^{-6}$
4^6	0	$-3.4\ 10^{-6}$	$-1.7\ 10^{-6}$	$2.8\ 10^{-5}$

Source: created by the authors.

For comparison, in Table 7 we present the errors obtained using the Courant functions.

Note. The C++ programs were developed for the numerical experiments in this paper.

Table 7 presents the errors of the Courant approximations on a sphere. The rows of these tables correspond to the levels of grid refinement (n is the number of triangles in the triangulation), and the columns correspond to the points ζ_{ki} with angular coordinates $(\frac{k\pi}{4} - \frac{\pi}{2}, \frac{\pi i}{2})$ at which the error is calculated.

Table 7. Errors in the Courant-type approximation of the function $f(x,y,z) = x$ defined on the unit sphere at points ζ_{ki} with angular coordinates $(\frac{k\pi}{4} - \frac{\pi}{2}, \frac{\pi i}{2})$

n	$\zeta_{1,1}$	$\zeta_{1,2}$	$\zeta_{1,3}$	$\zeta_{1,4}$
4^2	$-1.4\ 10^{-1}$	$1.6\ 10^{-1}$	$3.0\ 10^{-2}$	$-1.4\ 10^{-1}$
4^3	0	$4.8\ 10^{-2}$	$8.4\ 10^{-3}$	$-5.4\ 10^{-2}$
4^4	0	$8.6\ 10^{-3}$	$1.4\ 10^{-3}$	$-1.1\ 10^{-2}$
4^5	0	$2.8\ 10^{-3}$	$6.6\ 10^{-5}$	$-4.8\ 10^{-3}$
4^6	0	$8.0\ 10^{-4}$	$3.4\ 10^{-6}$	$-8.3\ 10^{-4}$

Source: created by the authors.

Comparing the results presented in Table 6 and Table 7, we see that the errors are smaller when approximating with Zlamal functions. This is consistent with theoretical results.

Paper [18] considers a special partition of the sphere into Voronoi cells in which the generating elements of the cells coincide with the centers of mass of those cells, as determined by a given density function.

Various methods for approximating functions on a sphere are known, such as Shepard's method, Moving Least Squares, and Radial basis functions. Shepard's method is frequently used for interpolation on a sphere. Shepard's method can function as either an exact or a smoothing interpolation method. The least-squares method is employed when constructing the interpolation function within local regions. The main disadvantages arise with large datasets: Shepard's method can be unstable. In such cases, the Modified Shepard's Method (MSM) is used. Instead of considering the entire dataset, the algorithm considers only the N nearest neighbors or points within a radius R, [19].

Radial Basis Function (RBF) interpolation and approximation provide an elegant and flexible method for reconstructing smooth fields from irregularly distributed spatio–temporal data [20].

The main idea in RBF approximation is to select m reference points (knots) $\xi_j, j = 1, \ldots, m$, where the precision of the data approximation is critical. In this case, the reference points must be carefully chosen [21], [22].

The main advantages are as follows: simplicity, no meshing required, flexibility, and smoothness. RBF interpolation typically results in a smooth and accurate approximation. A further advantage is independence from data domain dimensionality, although the interpolation error might be higher on the data domain border.

Using RBF leads to a system of linear equations: $Ax = b$, where the matrix A is of size $N \times N$, but is independent of the dimensionality of the data domain. However, the system of linear equations can be very large for large data sets.

The Courant and Zlámal approximations solve interpolation problems of the form $\tilde{U}(x_j) = U(x_j)$. We can consider a problem with a perturbation of the right-hand side:

$$\tilde{U}_{eps}(x_j) = U(x_j) + eps(x_j).$$

When constructing the Courant and Zlámal methods, the constant in the approximation theorem

is independent of the polynomial degree and the chosen set of points.

Therefore, the approximation error in the local region is as follows:

$$\| \widetilde{U}_{eps}(x_j) - U(x_j) \| \leq C \max_j |eps(x_j)|,$$

where $C = \text{const}$ is independent of the h and eps.

However, the Courant and Zlamal approximations are best suited for approximation at discrete points. Higher-order approximations can be obtained using the Argyris or Bell approximations. The resulting values can then be connected using smooth spline-based curves. We note that it is not necessary to know the curvilinear elements on the surface of the sphere; it is sufficient to know only the vertex coordinates. It is sufficient here to use approximations on the plane.

4 Conclusion

This paper considers a generalization of Zlamal's approximation on the plane and on the sphere. Comparison of the results of applying the Courant and Zlamal functions highlights the advantage, in terms of approximation error, of using the Zlamal functions. This confirms theoretical estimates of the approximation. In future papers, we will consider other variants of approximations on other manifolds with more attention to the computational work required for achieving specified accuracy.

Acknowledgement:
The authors are grateful to Yu. K. Dem'yanovich for consultations and mentoring.
The authors acknowledge Saint-Petersburg State University for research project 157438120.

Declaration of Generative AI and AI-assisted Technologies in the Writing Process

During the preparation of this work, the author(s) utilized artificial intelligence (AI) technologies solely for the purpose of linguistic refinement and grammatical correction. Following the application of these tools, the author(s) comprehensively reviewed, verified, and edited the resulting text. The author(s) maintain full accountability and responsibility for the accuracy, integrity, and final content of the publication.

References:

[1] Jan Franců & Michal Křížek, 100 years since the birth of Professor Miloš Zlámal, *Applications of Mathematics*, Published: 20 January 2026**,** Vol. 71, 2026, pp. 127–135, https://doi.org/10.21136/AM.2026.0273-25.

[2] J. H. Bramble, M. Zlámal, Triangular elements in the finite element method, *Math. Comput*., Vol.24, 1970, pp. 809–820.

[3] M. Zlamal, Curved elements in the finite element method. Time dependent problems, *Čisl. Met. Mech. Spl. Sredi*, Vol. 4, 1973, pp.25–49.

[4] Ciarlet, P. G. *The Finite Element Method for Elliptic Problems*. Classics in Applied Mathematics, Vol. 40. Philadelphia: Society for Industrial and Applied Mathematics (SIAM), 2002. ISBN 978-0-89871-514-9.

[5] M. Zlamal: On the finite element method, *Numer. Math*., Vol.12, 1968, pp.394–409.

[6] M. Zlámal: A finite element procedure of the second order of accuracy, *Numer. Math*. Vol. 14, 1970, 394–402.

[7] de Prenter, F., Verhoosel, C.V., van Brummelen, E.H. et al., Stability and Conditioning of Immersed Finite Element Methods: Analysis and Remedies, *Arch Computat Methods Eng* 30, 2023. pp.3617–3656. https://doi.org/10.1007/s11831-023-09913-0

[8] Giacomo Rizzieri, Simone Meni, Massimiliano Cremonesi, Liberato Ferrara, A Particle Finite Element Method for investigating the influence of material and process parameters in 3D Concrete Printing, *Computers & Structures*,Vol. 316, 2025, 10788 3, https://doi.org/10.1016/j.compstruc.2025.107883.

[9] Kevin Tannhäuser, Prince Henry Serrao, Sergey Kozinov, A three-dimensional collocation finite element method for higher-order electromechanical coupling, *Computers & Structures*, Vol. 291, 2024, 107219, ISSN 0045-7949, https://doi.org/10.1016/j.compstruc.2023.107219.

[10] Seddik, Mohamed S., Jehan Shazly, and Magdy B. Eteiba. 2024. Thermal Analysis of Power Transformer Using 2D and 3D Finite Element Method, *Energies* Vol.17, no. 13: 3203. https://doi.org/10.3390/en17133203

[11] Striska, L., Astrauskas, R., Kozulinas, N., Udris, D., Tolvaisiene, S., Macerauskas, E., Morkvenaite, I., & Ramanavicius, A.. Analysis of the Hertz Contact Model for Evaluating Mechanical Properties of Polymers Using the Finite Element Method, *Polymers*,

Vol. 17, no 22, 2025, 3018. https://doi.org/10.3390/polym17223018.

[12] Güvercin, Y., Yaylacı, M., Dizdar, A., Özdemir, M.E., Ay, S., Yaylacı, E.U., Karahasanoğlu, U., Uygun, H. and Peker, G. (2025), Biomechanical Analysis and Solution Suggestions of Screw Replacement Scenarios in Femoral Neck Fracture Surgeries: Finite Element Method. *Orthop Surg*, Vol.17: pp.614-623. https://doi.org/10.1111/os.14337.

[13] Izadi, Mohammad, Hari Mohan Srivastava, and Mahdi Kamandar. The LDG Finite-Element Method for Multi-Order FDEs: Applications to Circuit Equations," *Fractal and Fractional*, 9, no. 4: 230, 2025. https://doi.org/10.3390/fractalfract9040230.

[14] Vincenzo Biscotti, Rinto Roy, Marco Gherlone,Shape monitoring of morphing wing structures using the inverse Finite Element Method, *Computers & Structures*, Vol. 309, 2025, 107652, ISSN: 0045-7949, https://doi.org/10.1016/j.compstruc.2025.107652.

[15] Arif Muhammad Shoaib , Abodayeh Kamaleldin , Nawaz Yasir , The modified finite element method for heat and mass transfer of unsteady reacting flow with mixed convection, *Frontiers in Physics*, Vol. 10, 2022, ISSN:2296-424X. DOI: 10.3389/fphy.2022.952787.

[16] I.G.Burova, N.A. Lebedinskaya, D.M. Lebedinski, Approximations on Convex Star-Type Manifolds, 2026, *WSEAS Transactions on Computer Research, 14, pp. 705-713.* ISSN: 1991-8755 https://doi.org/10.37394/232018.2026.14.59.

[17] (*in Russian*) Yu.K. Dem'yanovich, *Local Approximation on Manifolds and Minimal Splines*, St. Petersburg State University Press, 1994. ISBN: 5-288-00481-1.

[18] Qiang Du, Max D. Gunzburger, Lili Ju, Voronoi-based finite volume methods, optimal Voronoi meshes, and PDEs on the sphere, *Comput. Methods Appl. Mech. Engrg.*, 192 2003, pp. 3933–3957.

[19] R. Cavoretto & A. De Rossi, Fast and accurate interpolation of large scat-tered data sets on the sphere, *J. Comput. Appl. Math*. 234, 2010, 1505–1521.

[20] Michal Smolik and Vaclav Skala. Radial basis function and multi-level 2D vector field approximation, *Mathematics and Computers in Simulation*, 181, 2021, pp. 522–538. issn: 0378-4754. doi: 10.1016/j.matcom.2020.10.009

[21] Martin Cervenka, Michal Smolik, and Vaclav Skala, A New Strategy for Scattered Data Approximation Using Radial Basis Functions Respecting Points of Inflection. *Lecture Notes in Computer Science* 11619 LNCS, 2019, pp. 322–336, Faro, Portugal, June 12–14, 2019 issn: 0302-9743. doi:10.1007/978-3-030-24289-3_24.

[22] Zuzana Majdisova, Vaclav Skala, and Michal Smolik, Algorithm for placement of reference points and choice of an appropriate variable shape parameter for the RBF approximation, *Integrated Computer-Aided Engineering*, 27.1, 2019, pp. 1–15. ISSN: 1069-2509. doi: 10.3233/ICA-190610.

Contribution of Individual Authors to the Creation of a Scientific Article (Ghostwriting Policy)

The authors equally contributed in the present research, at all stages from the formulation of the problem to the final findings and solution.

Sources of Funding for Research Presented in a Scientific Article or Scientific Article Itself

No funding was received for conducting this study.

Conflict of Interest

The authors have no conflicts of interest to declare that are relevant to the content of this article.

Creative Commons Attribution License 4.0 (Attribution 4.0 International, CC BY 4.0)

This article is published under the terms of the Creative Commons Attribution License 4.0
https://creativecommons.org/licenses/by/4.0/deed.en_US